

Efflux pump gene amplifications bypass necessity of multiple target mutations for resistance against dual-targeting antibiotic

Kalinga Pavan T. Silva, Ganesh Sundar, Anupama Khare*

Laboratory of Molecular Biology, National Cancer Institute, National Institutes of Health,
Bethesda, MD 20892, USA

*Correspondence: anupama.khare@nih.gov

Abstract

The rise of antimicrobial resistance has motivated the development of antibiotics that have multiple cellular targets, to theoretically reduce the frequency of resistance evolution, but adaptive trajectories and genetic determinants of resistance against such antibiotics are understudied. Here we investigate these in methicillin resistant *Staphylococcus aureus* (MRSA) using experimental evolution of ten independent populations in the presence of delafloxacin (DLX), a novel fluoroquinolone that targets both DNA gyrase and topoisomerase IV. We show that coding sequence mutations and genomic amplifications of the gene encoding a poorly characterized efflux pump, SdrM, lead to the evolution of high DLX resistance, circumventing the requirement for mutations in the target enzymes. Almost all of our evolved populations had one of two SdrM coding sequence mutations, which led to moderate DLX resistance. Additionally, these populations had 13 distinct genomic amplifications, each containing *sdrM* and two adjacent genes encoding efflux pumps, which resulted in up to 100-fold higher DLX resistance. While increased *sdrM* expression provided the selective advantage of the amplification in the DLX evolution, the adjacent efflux pumps hitchhiking in the genomic amplification contributed to cross-resistance against the aminoglycoside streptomycin. Finally, lack of *sdrM* necessitated mutations in both DNA gyrase and topoisomerase IV to evolve DLX resistance, and the presence of *sdrM* thus increased the frequency of resistance evolution. Our study highlights that instead of reduced rates of resistance, evolution of resistance to antibiotics with multiple cellular targets can involve alternate high-frequency evolutionary paths such as genomic amplifications of efflux pumps, that may cause unexpected alterations of the fitness landscape, including antibiotic cross-resistance.

Introduction

The emergence of antimicrobial resistance (AMR) is a major threat to global health. A recent report indicated that there may have been more than one million deaths worldwide due to AMR in 2019 (1). Methicillin resistant *Staphylococcus aureus* (MRSA) causes a wide-range of healthcare- and community-associated infections, with high incidence and mortality rates, and can attain resistance against most available antibiotics (2-7). Resistance determinants in bacteria are typically acquired either via horizontal gene transfer or *de novo* mutations, and mechanisms include antibiotic degradation or sequestration, modification of target components, and overproduction of efflux pumps (8-11). Additionally, ubiquitous, and unstable genomic duplications and amplifications can lead to increased expression of modifying enzymes and efflux pumps that then confer antibiotic resistance and may be selected for upon antibiotic exposure (12-14).

One strategy that has been proposed to reduce the rise of antibiotic resistance is to develop antibiotics with more than one target, thereby reducing the frequency of resistance evolution (15, 16). Recent studies have identified two such dual-targeting antibiotics that target membrane integrity as well as an additional cellular pathway and have so far avoided the emergence of resistance in the laboratory (17-19). The bacterial topoisomerases, DNA gyrase and topoisomerase IV, have also been proposed as potential targets for dual-targeting antibiotics, and it has been shown that targeting both enzymes may inhibit resistance evolution, and potentially involve novel resistance determinants (15, 16, 20, 21). However, the mechanisms of resistance evolution to such multi-targeting antibiotics and the underlying adaptive trajectories have not been characterized.

Fluoroquinolones are a widely-used class of antibiotics, and most traditional fluoroquinolones, such as ciprofloxacin and levofloxacin preferentially target either DNA gyrase or topoisomerase IV (22). Delafloxacin (DLX) is a 4th generation fluoroquinolone antibiotic, which targets both the DNA gyrase and topoisomerase IV enzymes with similar potency (23-25). Due

to this dual-targeting, it was thought that resistance against DLX might be infrequent (24, 26, 27), but DLX resistance has recently been observed in clinical isolates of MRSA (28).

In this study we investigate the evolution of MRSA resistance to dual-targeting antibiotics, using experimental evolution of multiple independent MRSA populations in increasing concentrations of DLX. We observe that in addition to mutations in the DNA gyrase and topoisomerase IV enzymes, coding sequence mutations in the major facilitator superfamily efflux pump *SdrM* (*Staphylococcus drug resistance*), and genomic amplifications of *sdrM* and the neighboring efflux pumps *sepA* and *lmrS* are widespread in the evolved populations, and typically evolve earlier than the canonical mutations. The *sdrM* coding sequence mutations confer moderate DLX resistance, and increase evolvability of such resistance, while the genomic amplifications lead to high DLX resistance. Copy number variation of the amplified region is dependent on the selective pressure and causes population heterogeneity for DLX resistance. We find that while *sdrM* activity provides the fitness advantage for selection of these genomic amplifications upon DLX exposure, hitchhiking of the neighboring efflux pumps in the genomic amplification leads to cross-resistance against the aminoglycoside streptomycin. Finally, we show that in the absence of *sdrM* activity, DLX resistance requires mutations in both the DNA gyrase and topoisomerase IV enzymes, and thus arises at a lower frequency.

Results

Multiple evolved MRSA populations likely have novel determinants of DLX-resistance

We evolved ten independent populations of the MRSA strain JE2 in increasing concentrations of DLX for 7-10 daily passages. DLX inhibits both the DNA gyrase and topoisomerase IV enzymes with similar potency raising the possibility that resistance to DLX may develop infrequently (27). However, all ten populations were able to grow in DLX concentrations that were 64-1024x the minimum inhibitory concentration (MIC) of the parental JE2 strain (**Supplementary Table 1, see Materials and Methods for strain nomenclature**). The JE2 strain

had an MIC of 0.133 ± 0.027 $\mu\text{g/ml}$, which is below the clinical breakpoint of 0.25 $\mu\text{g/ml}$ (23-25). Three individual isolates from the terminal passage of each evolved population showed DLX MICs ranging between ~ 2 - 33 $\mu\text{g/ml}$ (**Supplementary Figure 1A**), confirming the evolution of high DLX resistance. We carried out whole genome sequencing on these isolates, as well as additional isolates and populations from earlier passages of the evolution (**Supplementary Table 2**). As expected, most of the resistant strains had mutations in genes encoding the subunits of either DNA gyrase (*gyrA* or *gyrB*) or topoisomerase IV (*parC* or *parE*) or both (**Figure 1**). Most of the single nucleotide polymorphisms (SNPs) that arose in these canonical targets such as S85P and E88K in *gyrA*, R458L in *gyrB*, E84K and A116V in *parC*, and D432G and P585S in *parE* are located in the quinolone resistance determining region (QRDR) of these proteins and have been previously associated with fluoroquinolone resistance (26, 29-32). We also identified other mutations such as W592R in *gyrB*, S520R in *parC* and S437P in *parE* in our mutants, which may be novel DLX resistance alleles.

Despite the numerous canonical target mutations, several resistant isolates as well as populations from intermediate passages of most of the ten independent populations did not carry any canonical mutations in genes coding for either the DNA gyrase or topoisomerase IV enzymes or had mutations in only one of the targets (**Figure 1 and Supplementary Table 2**). These include all samples from populations 1, 3, and 6, as well as the populations from multiple early passages of populations 2, 4, 5, 7, 8, and 9. Evolved *gyrA** (*gyrA*^{E88K}) or *parE** (*parE*^{D432G}) mutant alleles individually led to a very mild increase in DLX MICs up to 0.4 $\mu\text{g/ml}$ (**Supplementary Figure 1B**) suggesting that other genes likely play a role in DLX resistance in several of our evolved populations.

Efflux pump mutations and gene amplifications were prevalent in the evolved mutants

Further examination of our whole-genome sequencing results revealed that mutations in the efflux pump SdrM (*Staphylococcus* drug resistance) were common in the evolved populations

(Figure 1). SdrM is an efflux pump from the major facilitator superfamily (MFS) (33). Overexpression of SdrM has been shown to confer a 2-fold increase in norfloxacin and ethidium bromide MICs, however this efflux pump has not been implicated in the evolution of antibiotic resistance (33). Contrary to typical efflux pump mutations that occur in the promoter region (or in a repressor), we observed that strains in eight out of the ten evolved populations contained one of two *sdrM* coding sequence mutations, Y363H (*sdrM1*^{*}) or A268S (*sdrM2*^{*}), but none of the strains had both (**Figure 1, Supplementary Table 2**), raising the possibility that these two mutations might have similar functionality. Population 6 had a mutation upstream of the *sdrM* coding sequence (at the -164 position) which may affect the regulation of *sdrM* expression, in addition to the A268S mutation (*sdrM3*^{*}).

Alignment of the SdrM amino acid sequence with other known MFS efflux pumps using the Conserved Domain Database (34) showed that the A268 and Y363 residues are likely situated in the binding pocket of the SdrM efflux pump (**Supplementary Figure 2**), suggesting that the mutations affect binding of SdrM to DLX. Visualization of the predicted protein structure of SdrM using AlphaFold (35, 36), indicated that A268 and Y363 are in close proximity to each other (**Supplementary Figure 3**).

In addition to the *sdrM* alleles, coverage analysis of the whole-genome sequencing results revealed that the coverage of the *sdrM* gene was 2-5-fold higher than the mean coverage of the genome in multiple evolved mutants, compared to ~1X coverage in the WT, indicating an amplification of the *sdrM* gene across all ten evolved populations (**Figure 1, Supplementary Table 2**).

***sdrM* mutant alleles increase DLX resistance and efflux, and evolvability of DLX resistance**

We constructed individual *sdrM* allele-replacement mutants in the wild-type (WT) JE2 strain and determined the effect of the evolved alleles on DLX resistance and efflux. Strains with the *sdrM1*^{*} or *sdrM2*^{*} alleles showed a ~2-fold increase in DLX resistance, while those carrying

the *sdrM3** allele (that consists of both an intergenic and coding sequencing mutation) showed a ~4-fold increase (**Figure 2A**). We measured the intrinsic fluorescence of DLX (37) to indirectly determine the intracellular concentration of DLX and calculated the rate of efflux in the three allelic replacement mutants, as well as the WT and a mutant with a transposon insertion in *sdrM* (*sdrM::Tn*) as controls (**Figure 2B**). As expected, the WT and *sdrM::Tn* strains had the highest intracellular DLX concentrations, while the three allele-replacement mutants had lower levels, suggesting that the evolved *sdrM* alleles led to increased efflux. Using a simplified mathematical model, we determined that the rates of DLX efflux of *sdrM1**, *sdrM2** and *sdrM3** were ~2-9x higher than *sdrM::Tn*, while the WT rate was similar to *sdrM::Tn*. (**Supplementary Figure 4**).

From our whole-genome sequencing results, we observed that in eight out of the ten evolved populations *sdrM* mutations (either a SNP or the amplification) emerged at an earlier passage compared to the canonical DNA gyrase or topoisomerase IV mutations (**Figure 1**). This suggests an evolutionary cascade in which efflux pump mutations facilitate the selection of canonical mutations for DLX resistance. To test if *sdrM* mutations can affect the evolvability of resistance in the presence of DLX, we evolved 12 independent populations each of WT, *sdrM::Tn*, and strains carrying the individual *sdrM* evolved alleles for 14 days in a DLX concentration (2 µg/ml) that was higher than the MICs of all the allelic replacement strains. While none of the WT and *sdrM::Tn* populations were able to evolve resistance over the duration of the experiment, all *sdrM3** populations, and a smaller fraction of *sdrM1** and *sdrM2** populations, evolved resistance (**Figure 2C**). Considering the possibility that the DLX concentration might be too high for the WT and *sdrM::Tn* strains, we conducted a similar experiment at a lower DLX concentration (0.75 µg/ml). Since this DLX concentration was similar to the MIC for *sdrM3**, we did not include this strain in the experiment. All *sdrM1** and *sdrM2** populations, but none of the WT or *sdrM::Tn* populations, evolved resistance in 5 days (**Figure 2D**), indicating that the evolved *sdrM* alleles can promote the evolution of DLX resistance.

Efflux pump gene amplifications play a role in DLX resistance

In addition to the point mutations in *sdrM*, we identified 13 distinct types of amplifications from our whole-genome sequencing data across our ten evolved populations, that amplified the *sdrM* gene (**Figures 1 and 3A, Supplementary Table 3, Supplementary Figure 5**). At least one instance of each amplification type was confirmed via PCR and Sanger sequencing of the novel junctions. One end of every amplification was within an rRNA-tRNA gene cluster located downstream of *sdrM* (terminal 1), while the other end was either within or between the five genes upstream of *sdrM* (terminal 2) (**Figure 3A**). While five of these amplifications had microhomology of 4-12 base pairs between the two terminals, the others had either a single base-pair homology or none (**Supplementary Table 3**). Several of the amplifications were found in multiple populations and in some populations, different amplifications were seen in different passages, indicating that the amplifications are dynamic (**Supplementary Figure 6**). The *sdrM* gene is present upstream of two additional efflux pumps *sepA* and *ImrS* (38, 39), and both these genes were present within the amplifications in all cases (**Figure 3A**). Gene neighborhood analysis using the STRING database (40) indicated that the three efflux pumps (along with a hemolysin III family protein) are found next to each other in the genome in almost all *Staphylococcus* species (**Supplementary Figure 7**).

To further characterize the effects of the genomic amplifications, we analyzed three evolved isolates that contained only non-canonical mutations – 1.7a, 4.2a and 6c. All three isolates were predicted to have efflux pump amplifications, where 1.7a had amplification type 9 and both 4.2a and 6c had amplification type 1 (**Figure 3B, Supplementary Table 3**). While 4.2a had the WT *sdrM* allele, 1.7a had the *sdrM2** allele, and 6c had ~40% reads mapping to the *sdrM3** allele in the whole-genome sequencing data, suggesting that the amplification contained both WT and *sdrM3** alleles. Additionally, 1.7a and 6c had mutations in a few other non-canonical genes, but these mutations did not affect resistance to DLX (**Supplementary Table 2, Supplementary Figure 8**).

The *sdrM*, *lmrS*, and *sepA* genes showed a 3-10-fold increase in copy number in 1.7a, 4.2a, and 6c, while a control strain, 3a, that was predicted to not have the amplification, showed a similar copy number to the WT, as measured by genomic DNA qPCR (**Figure 3B, 3C**). Further, the three strains showed a 5-500-fold increase in gene expression of the three efflux pumps compared to the WT strain, as measured by quantitative reverse transcription PCR (RT-qPCR) (**Figure 3D**). The dramatically higher expression compared to the copy number, especially in 1.7a and 4.2a, likely reflects altered regulation of the efflux pumps in the amplifications. All three strains had ~5-100-fold higher DLX resistance and high DLX efflux compared to the parental WT strain (**Figure 3E, 3F**).

To test whether the overexpression of the amplified efflux pumps individually, or in combination, can increase DLX resistance, we overexpressed *sepA*, *lmrS*, or the parental and evolved *sdrM* alleles under the control of the corresponding native promoters using the pKK30 plasmid (41). In these strains, the expression of the efflux pumps increased ~10-100 fold compared to an empty vector control (**Supplementary Figure 9A**). Overexpression of the WT *sdrM* allele led to a ~2-fold increase in DLX efflux activity and resistance, while the *sdrM1**, *sdrM2**, and *sdrM3** alleles showed a ~4-6-fold increase (**Supplementary Figure 9B, 9C**). Further, overexpression of *sepA* and *lmrS* did not lead to a significant increase in DLX resistance, and overexpression of all 3 efflux pumps led to similar resistance as overexpression of the WT *sdrM* allele indicating that *sdrM* overexpression is likely the main contributor to DLX resistance caused by the genomic amplifications (**Supplementary Figure 9B**).

Amplification copy number increases upon antibiotic exposure and leads to cross-resistance

Amplification instability commonly causes changes in copy number, and consequently expression, which may depend on the selective strength of environmental conditions (12, 14). To test the stability of the amplification, we passaged 1.7a and 6c in two concentrations of DLX, as

well as antibiotic-free media, for two days and determined the *sdrM* read coverage for each passage using whole-genome sequencing. The copy number of *sdrM* increased upon passaging in DLX, and decreased upon passaging without the antibiotic, indicating that the *sdrM* copy number, and likely its expression, in the genomic amplifications is dependent on the level of DLX exposure (**Figure 4A, 4B**). Further, the frequency of the two mutations in the *sdrM3** allele (A268S coding sequence mutation and an upstream mutation) in 6c increased upon DLX passaging and decreased upon passaging in the antibiotic-free media (**Figure 4A**). The strains that had been passaged for two days in the higher concentration of DLX, and had higher amplification copy number, also showed a ~2-fold increase in DLX resistance for 6c, and a mild increase for 1.7a (**Figure 4C, 4D**).

Given the presence of three efflux pumps in the amplification, and their resulting high expression, we tested the resistance of 1.7a grown with and without DLX, against a panel of different antibiotics. While we did not see increased resistance against most antibiotics, 1.7a grown in DLX showed cross-resistance against the aminoglycoside streptomycin (**Figure 4E**). Further, overexpression of all three efflux pumps, but not *sdrM* alone, resulted in a similar increase in streptomycin resistance (**Figure 4F**), indicating that streptomycin resistance also required increased expression of *ImrS* and *sepA*.

***sdrM* is required for selection of amplifications and increases evolvability of DLX resistance**

To understand the role of *sdrM* in the selection of the genomic amplifications, we evolved three independent populations each of the transposon mutant strain *sdrM::Tn* and WT (as a control), in increasing concentrations of DLX, similar to our original evolution. The *sdrM::Tn* strain has an MIC ~2-fold lower than the WT (**Figure 5A**), indicating that SdrM contributes to the intrinsic DLX resistance level of the WT MRSA strain. During the evolution, the populations grew in DLX concentrations ~640-1000 times the respective MICs. We saw genomic amplifications of the *sdrM*

locus in 2 out of the 3 independent WT populations, while the 3rd population also showed junctions associated with the amplification, but the copy number increase was lower than our 1.3-fold threshold. Each WT population had a novel amplification type not seen in the original evolution (**Supplementary Table 3**). However, none of the *sdrM*::Tn populations had these amplifications (**Figure 5B**). Further, unlike the WT populations, all sequenced populations from the intermediate and terminal passages of the *sdrM*::Tn evolutions had mutations in both the DNA gyrase and topoisomerase IV enzymes, suggesting that the high DLX resistance was due to stable target mutations, as opposed to amplifications (**Figure 5B**).

Amplifications are known to be unstable and commonly underlie antibiotic heteroresistance in populations (42, 43), while resistance due to changes in DNA sequence is predicted to be more stable and homogenous. We therefore tested the population heterogeneity for antibiotic resistance in the evolved isolates 1.7a and 6c that have genomic amplifications but no canonical target mutations, as well as an isolate from the final passage of an evolved *sdrM*::Tn population that has mutations in *gyrA*, *gyrB*, and *parE* (**Figure 5B, Supplementary Table 2**). We grew the strains overnight in antibiotic-free media and then determined the fraction of the population that could grow in different DLX concentrations. We observed that while the *sdrM*::Tn evolved isolate (Tn_3b) showed ~100% DLX resistance at all concentrations tested, 1.7a and 6c showed population heterogeneity, where only ~10% or fewer cells were resistant to DLX (**Figure 5C**).

The presence of mutations in both target enzymes in all evolved *sdrM*::Tn populations (**Figure 5B**) suggested that in the absence of *sdrM*, mutations in both targets are essential for high DLX resistance. We therefore tested whether the presence of *sdrM* affected the evolvability of DLX resistance. We evolved 12 independent populations each of the WT and *sdrM*::Tn in fixed concentrations of DLX that were 2.5x the respective MIC for each strain (0.55 µg/ml for WT and 0.32 µg/ml for *sdrM*::Tn). While 5 of the 12 WT populations evolved DLX resistance in 6 days,

only 1 of 12 *sdrM*::Tn populations evolved resistance in 8 days, indicating that the presence of *sdrM* increases the evolvability of DLX resistance (**Figure 5D**).

Discussion

Resistance against antibiotics with more than one cellular target likely requires multiple mutations in a cell and is thus predicted to be infrequent. However, the evolutionary paths leading to resistance against such antibiotics are not well-characterized. In this study, we showed that the evolution of MRSA upon exposure to the dual-targeting 4th generation fluoroquinolone DLX led to resistance via both coding sequence and upstream mutations in *sdrM*, the gene encoding a poorly characterized major facilitator superfamily efflux pump, as well as gene amplifications of *sdrM*. Further, the presence of two additional efflux pumps adjacent to the *sdrM* locus, and consequently their hitchhiking in the genomic amplification, led to cross-resistance against the aminoglycoside streptomycin. In the absence of *sdrM*, strains required mutations in both canonical targets, DNA gyrase and topoisomerase IV, to attain DLX resistance, and therefore had reduced evolvability of DLX resistance. The *sdrM* mutations and amplifications thus provided a more accessible adaptive path to high DLX resistance. Our results suggest that antibiotics with multiple targets may inadvertently lead to alternate adaptive trajectories that not only allow for rapid evolution of resistance, but also lead to additional unfavorable changes in the bacterial fitness landscape.

Efflux pumps are thought to provide rapid protection to cells upon antibiotic exposure, and efflux pump mutations are commonly associated with antibiotic resistance (44). Several efflux pumps from multiple protein families are present in MRSA. The MFS family pumps include chromosomally encoded NorA, NorB, NorC, LmrS, MdeA, and SdrM, and plasmid-based overexpression of these pumps can confer resistance to fluoroquinolones, quaternary ammonium compounds, and dyes (45, 46). While mutations in *norA* have been associated with the evolution of antibiotic resistance, especially against fluoroquinolones (47), *sdrM* mutations have not been previously implicated. Our study thus shows that less well-characterized efflux pumps may play

a role in the acquisition of antimicrobial resistance, especially against newly developed antimicrobials. Further, it had been previously suggested that plasmid-based overexpression of *ImrS* and *sepA* in *E. coli* or a methicillin-sensitive *S. aureus* strain could lead to increased resistance against multiple antibiotics including linezolid, erythromycin, and kanamycin (48-50). However, we did not observe cross-resistance against these antibiotics in our evolved isolates that overexpressed these efflux pumps, indicating that this resistance may be specific to *E. coli* or the strain of *S. aureus*.

Antibiotic-resistance associated efflux pump mutations typically increase the expression of the efflux pump, thereby reducing antibiotic concentrations within the cell. Such mutations are most often located either in the promoter region or in a repressor of the pump, although genomic amplifications of efflux pumps have also been observed (51, 52). In our evolutions, we did not identify any transcriptional repressor mutations that would increase *sdrM* expression, and only one population had a mutation upstream of *sdrM*, whereas *sdrM* amplifications were common in all ten independently evolved populations. This suggests that the substantial increase in *sdrM* expression required for high DLX resistance is largely inaccessible via promoter or repressor mutations. Expression levels of *sdrM* and the adjacent efflux pumps *ImrS* and *sepA* were much higher compared to the copy number of the coding genes suggesting that the regulation of these genes was altered in the amplification. Interestingly, a tRNA-rRNA gene cluster is located upstream of the amplified copies of the efflux pumps raising the possibility that read-through transcription from the cluster may result in the highly increased expression we observed in our evolved strains containing amplifications, similar to a previous observation in *Streptococcus pneumoniae* (52).

Coding sequence mutations in efflux pumps have also been shown to increase antibiotic resistance in *Pseudomonas aeruginosa* (*mexB*, *mexY*), *Klebsiella pneumoniae* (*kmrA*), and *Neisseria gonorrhoeae* (*mtrD*), likely due to increased affinity for the antibiotic (53-55). Recent studies have suggested that increased expression of efflux pumps could also facilitate antibiotic

resistance either by increasing the mutation rate (56, 57), allowing expression of resistance determinants upon plasmid acquisition (58), or promoting selection of resistance mutations due to increased fitness upon antibiotic exposure of strains both carrying the resistance mutations and overexpressing efflux pumps (59). We also found that coding sequence mutations in the SdrM binding pocket increased DLX resistance and efflux, likely by altering the binding to DLX. The *sdrM3** upstream mutation probably led to elevated levels of the *sdrM* efflux pump, which in turn led to a larger increase in DLX efflux and resistance. Further, the moderate increase in DLX resistance of the *sdrM* mutant alleles prompted increased evolvability of DLX resistance compared to the WT, which suggests that coding sequence efflux pump mutations might also be able to facilitate the evolution of higher levels of resistance, possibly due to a synergistic increase in resistance, or elevated fitness, of combination mutants. Finally, we showed that amplification of *sdrM* provided a single-step adaptive route to DLX resistance, while at least two mutations, in the DNA gyrase and topoisomerase IV enzymes, were necessary for high DLX resistance in the absence of *sdrM*, and the presence of a functional *sdrM* gene therefore increased the frequency of DLX resistance evolution. Since genomic amplifications are thought to be much more common than mutations in the genomic sequence (12, 14), it is likely that the combination of an *sdrM* coding sequence mutation and amplification also arose more frequently than the combination of coding sequence mutations in the two target enzymes. The few DLX resistant *S. aureus* clinical isolates that were identified and sequenced in a previous study had mutations in both the DNA gyrase and topoisomerase IV enzymes (60). However, these isolates were collected prior to DLX approval and clinical use and the selective pressures and mutational paths that led to the acquisition of the target mutations is therefore unknown.

Genomic duplications and amplifications are estimated to be present in 10% of bacterial cells in growing cultures and due to their high frequency, are thought to play an important role in the early adaptation to stress, including antibiotic resistance (12, 14). Our study demonstrates that genomic amplifications of efflux pumps can lead to antibiotic resistance and may be the first

steps of evolutionary paths that allow for the rapid evolution of more stable resistance mutations, especially when multiple such mutations are required for high levels of resistance.

Genomic amplifications are typically unstable and frequently lost in the absence of selective pressure, leading to population heterogeneity, and antibiotic heteroresistance (42, 43). We observed similar amplification instability in our study, leading to population heterogeneity of DLX resistance. Further, treatment with high concentrations of DLX led to increased amplification copy number, and consequently increased DLX resistance, as well as cross-resistance against streptomycin. Heteroresistance against fluoroquinolones was rarely seen in clinical isolates from four pathogens in a previous study and this was ascribed to resistance requiring target mutations (43). However, our study shows that in MRSA, genomic amplifications of efflux pumps can lead to high fluoroquinolone resistance. The instability of genomic amplifications likely leads to their under-detection in laboratory and clinical studies, and their role in antibiotic resistance is thus probably underappreciated.

Interestingly, 16 distinct genomic amplification types of *sdrM* were observed in our 13 independent WT populations, and the amplifications were dynamic within each population, further highlighting their instability. Further, we observed the same amplification arising and being selected for in multiple independent populations, suggesting that DNA breaks and amplifications may preferentially occur at certain genomic sites. The sequence of the amplification junctions consisted of either micro-homology of at most 13 bp, or no homology, which is less than the 20-40 bp threshold required for RecA-mediated recombination (14). This suggests that the initial duplication in our evolved populations likely occurred via random end-joining and may be RecA-independent.

DNA breaks contribute to the formation of genomic amplifications, both in bacteria as well as eukaryotic systems (14, 61). DNA gyrase and topoisomerase IV enzymes relieve topological stress in the DNA, generating short-lived DNA double-stranded breaks, that are then re-ligated. Fluoroquinolones typically bind DNA gyrase or topoisomerase IV in a complex with DNA and may

both promote DNA cleavage and strongly inhibit religation of the DNA ends, resulting in increased DNA double-stranded breaks (62, 63). Fluoroquinolone antibiotics may thus promote the formation of genomic amplifications, and in our study, we observed pervasive generation and selection of *sdrM*-containing genomic amplifications upon DLX exposure. A recent study also showed that genomic amplifications of an inhibitor protein in *Salmonella* Typhimurium and *Escherichia coli* evolved upon exposure to the DNA gyrase poison albicidin which also blocks DNA religation (64), and provided albicidin resistance, further indicating that inhibition of DNA topoisomerase enzymes may aid in the formation of genomic amplifications (65).

Multi-target antibiotics or drug combinations are thought to reduce the frequency of antibiotic resistance. However, our study indicates that if one of the targets of such treatments is the DNA gyrase or topoisomerase enzyme, it may instead select for gene amplifications that arise due to breaks in the DNA and lead to rapid evolution of resistance, and these amplifications may also lead to additional unanticipated fitness consequences, including cross-resistance. A better understanding of the genetic and environmental factors that affect genomic amplifications, as well as the adaptive trajectories that are accessible due to the selection of such amplifications, especially in clinical settings, is therefore necessary to inform new antimicrobial therapies.

Materials and Methods

Strains and growth conditions

All strains and plasmids used in this work are described in **Supplementary Table 4**.

All experiments in liquid media were carried out at 37°C, shaking at 300 rpm, in modified M63 media (66) (13.6 g/L KH₂PO₄, 2 g/L (NH₄)₂SO₄, 0.4 µM ferric citrate, 1 mM MgSO₄; pH adjusted to 7.0 with KOH) supplemented with 0.3% glucose, 0.1 µg/ml biotin, 2 µg/ml nicotinic acid, 1X Supplement EZ (Teknova) and 1X ACGU solution (Teknova), or in Mueller Hinton Broth 2 (MH2)

(Millipore sigma) with or without 1X ACGU. For cloning and strain construction, strains were grown in LB liquid media (10 g/L bacto-tryptone, 5 g/L yeast extract, 10 g/L NaCl) or on LB plates (containing 15 g/L agar), supplemented with the appropriate antibiotic (10 µg/ml chloramphenicol, 50 µg/ml ampicillin, 10 µg/ml trimethoprim) or 0.4% para-chlorophenylalanine (PCPA) for counter-selection. MH2 plates were made with MH2 agar (Millipore sigma) and supplemented appropriately with 1X ACGU and DLX (either 0.5, 1 or 2 µg/ml).

Laboratory evolution of DLX resistance

Ten independent populations of *S. aureus* JE2 cells were grown shaking at 300 rpm at 37°C, in the presence of increasing concentrations of DLX, with a daily 50-100-fold dilution into 14 ml snap-cap tubes containing 2 ml fresh media with DLX. The evolution was started between 0.05-0.25 µg/ml DLX, and the concentration was increased 2-fold at each exposure. Evolution was stopped at 128 or 256 µg/ml DLX, except for 2 populations which didn't grow after 2 attempts at 32 µg/ml and 64 µg/ml DLX respectively. Details of the populations are in **Supplementary Table 1**.

A similar setup was used to evolve the *sdrM*:Tn mutant, where three independent populations each of *sdrM*:Tn and WT were evolved in parallel, starting at a DLX concentration of 0.1 µg/ml, and the concentrations were increased 1.5-2-fold at each exposure. Evolution was stopped as described above.

Strain nomenclature

Each of the ten independently evolved populations from the initial evolution was labeled from P1-P10. Hence, P1 signifies the 1st independently evolved population. We introduce a dot and a second number which represents the passage number, for example, P1.7 indicates the 7th passage of the 1st evolved population. The letters appearing at the end of each number indicate that it was an isolate, for instance, 1.7a indicates an isolate extracted from population P1.7. The

isolates from the final passage are represented as the population number and a letter, for example 1a is an isolate from the final passage in population P1.

Whole-genome sequencing of evolved populations and isolates

Genomic DNA was prepared from selected populations and isolates using the Qiagen DNeasy Blood and Tissue kit. Then, indexed single-end or paired-end libraries were prepared using the Illumina Nextera XT DNA Library Preparation kit and sequenced either on an Illumina MiSeq or Nextseq 500 sequencer. The data were analyzed as described before (67, 68), where the Illumina adapters were removed using *cutadapt* (69), the reads were trimmed with *trimmomatic* (70), or both steps done using *fastp* (68), and the mutations in the evolved populations were identified using *breseq* (71). The mutations identified in the evolved populations in genes encoding the canonical targets or efflux pumps compared to the parental strain are listed in **Supplementary Table 2**.

Determination of genomic amplification copy number

The coverage depth of each base pair in the whole-genome sequencing data was determined using the BAM2COV command in *breseq*. The coverage of all base pairs was summed for the whole genome or each gene of interest and then was divided by the sequence length (number of base pairs). The fold change in coverage was then determined by dividing the corresponding number of reads per base pair of the gene with that of the whole genome. To identify *sdrM* amplifications, samples had to have a genomic junction which led to *sdrM* amplification (as determined by *breseq*) and meet a threshold for relative read coverage of *sdrM*. For isolates, the relative coverage of *sdrM* had to be at least 2x the mean WT value (from three biological replicates), while for populations, the relative *sdrM* coverage had to be at least 1.3x the mean WT coverage (to allow for population heterogeneity). For each amplification type, at least one instance was verified by PCR amplification of the novel junction followed by Sanger sequencing.

Construction of allele-replacement mutants

Genomic DNA was extracted from mutant isolates, and the mutated alleles were amplified through PCR and cloned into pIMAY* digested with BamHI and EcoRI, using Gibson assembly (72). The methylation profile of the plasmids was matched to *S. aureus* after electroporating and extracting the constructed plasmids from *E. coli* IM08B (73). Plasmid extraction was done using Qiagen Plasmid MIDI kit and the plasmids were concentrated using Savant SpeedVac SPD1030. Allelic replacement was carried out in *S. aureus* JE2 as described (72). Briefly, plasmids were electroporated into *S. aureus* JE2 cells and plated at 30°C on LB Agar + chloramphenicol. Transformed colonies were grown shaking at 37°C in LB media + chloramphenicol for two overnights, with a 1:1000 dilution into fresh medium after the first overnight. The following day the cells were plated on LB Agar + chloramphenicol, and colonies were tested for integration by PCR with integration primers listed in **Supplementary Table 5**. For plasmid excision, colonies which showed integration were grown in LB media at 25°C with shaking for two overnights, with a 1:1000 fold-dilution after the first overnight. Cells were then plated on LB plates containing 0.4% para-chlorophenylalanine (PCPA), and colonies were screened based on the size, with larger sizes assumed to indicate plasmid excision. 60-100 large colonies were streaked onto LB plates with and without chloramphenicol to identify chloramphenicol-sensitive clones. Presence of the mutant allele was confirmed by Sanger sequencing using the sequencing primers (see **Supplementary Table 5**).

Construction of overexpression strains

To construct the overexpression strains, WT genes and *sdrM* mutant alleles were amplified by PCR and cloned into PCR amplified pKK30 vector using Gibson assembly. The Gibson assembled product was electroporated into *E. coli* DH5 α λ -pir electrocompetent cells and recovered on LB Agar + trimethoprim plates. Plasmids were extracted from the *E. coli* strains and

electroporated into *S. aureus* RN4220. Plasmids were extracted once more and electroporated into *S. aureus* JE2.

Efflux assay

Cells were grown for 16 hours in 2 ml of M63. 2 μ l of these cells were added to 198 μ l of M63 + 0.1 μ g/ml DLX in a 96-well plate. The fluorescence of DLX (excitation and emission wavelengths of $\lambda_{exc} = 395$ nm and $\lambda_{em} = 450$ nm respectively) (37), and the OD₆₀₀ were measured every 30 minutes for 22 hours. Data from the final 12 hours are shown in the figures. As controls, readings were taken for cells in M63 with no DLX or 0.1 μ g/ml DLX, and M63 alone. The normalized fluorescence (fluorescence/OD₆₀₀) was calculated as,

$$\frac{(\text{Fluor. of cells in M63 + DLX}) - (\text{Fluor. of M63 + DLX})}{(\text{OD}_{600} \text{ of cells in M63 + DLX}) - (\text{OD}_{600} \text{ of M63 + DLX})} - \frac{(\text{Fluor. of cells in M63}) - (\text{Fluor. of M63})}{(\text{OD}_{600} \text{ of cells in M63}) - (\text{OD}_{600} \text{ of M63})}$$

Model to determine the rate of DLX efflux

To determine the rates of DLX efflux, we considered a simplified mathematical model to only capture the increase in the DLX concentration inside the cells. Given the selection of *sdrM* mutations, and the effect of *sdrM* overexpression on DLX resistance, we assumed that DLX efflux was mainly dependent on SdrM activity. We defined the following differential equations:

$$\frac{dC_{in}}{dt} = \rho_{in}C_{out} - \rho_{out}C_{in}$$
$$\frac{dC_{out}}{dt} = A - \rho_{in}C_{out} + \rho_{out}C_{in}$$

where, C_{in} is the DLX concentration inside the cell at time t , ρ_{in} is the rate of influx of DLX in to the cell, C_{out} is the DLX concentration outside of the cell at time t , ρ_{out} is the rate of efflux of DLX out of the cell and $A = C_{out}(t = 0)$ is the initial DLX concentration we used for the experiment,

0.1 $\mu\text{g/ml}$ ($\sim 0.226 \mu\text{M}$). We assumed that DLX binding, and unbinding occurs very fast, and do not take it into account in our equations for simplicity. Solving the two equations above we get:

$$\frac{d^2 C_{in}}{dt^2} + (\rho_{in} + \rho_{out}) \frac{dC_{in}}{dt} - \rho_{in} A = 0$$

Integrating this second order linear ordinary differential equation with $C_{in}(t = 0) = 0$ we get,

$$C_{in} = \frac{1}{(\rho_{in} + \rho_{out})} (B (e^{-(\rho_{in} + \rho_{out})t} - 1) + \rho_{in} A t)$$

where B is an arbitrary constant. As the normalized fluorescence we determined with the efflux assay was a proxy to C_{in} , we performed a least-squared fit of C_{in} with the normalized fluorescence vs time for *sdrM::Tn*, to determine B and ρ_{in} , assuming that the rate of efflux will be equal to the rate of influx, $\rho_{in} = \rho_{out}$ for the transposon mutant since SdrM is absent and the transport of DLX into and out of the cell will be passive. The best fit values for B and ρ_{in} were assumed to be the same for the other strains. Substituting these values, we performed least-squared fit for WT, *sdrM1**, *sdrM2**, and *sdrM3** to determine the best fit values for the efflux rates ρ_{out} for each strain. As we were fitting C_{in} to the normalized fluorescence, the units of the rates of influx and efflux were arbitrary units/time (hours).

Measurement of MICs

DLX was serially diluted 2-fold in a Corning 96-well flat clear bottom plate, to obtain eight concentrations. Cells grown overnight in M63 media or Mueller Hinton Broth 2 (MH2) were transferred at a final dilution of 1:5000 to the 96-well plate containing the serially diluted antibiotic and grown at 37°C with shaking for 24 hours. After growth, the OD_{600} was measured using a plate reader. The data points were fitted to a modified Gompertz function to determine the minimum inhibitory concentrations (74). To determine the multidrug MICs, WT was grown in MH2 broth supplemented with 1X ACGU, and 1.7a was grown in MH2 supplemented with 1X ACGU with or without 2 $\mu\text{g/ml}$ DLX overnight. The following day, all three overnights were washed twice in 1x

PBS and the MICs for all antibiotics were determined. MH2 medium was supplemented with 1X ACGU for experiments with 1.7a, as *pyrC*, a gene involved in pyrimidine synthesis, had a frameshift mutation in 1.7a, resulting in poor growth without 1X ACGU supplementation.

Quantitative PCR (qPCR)

Genomic DNA was extracted as described above. RNA was extracted from cells grown overnight in M63 using the Total RNA Purification Plus Kit (Norgen Biotek Corp) and DNA was removed using the TURBO DNA-free™ Kit (Invitrogen). cDNA was synthesized using random primers and Superscript III Reverse Transcriptase (Thermo Fisher Scientific). Genomic DNA or cDNA were mixed with primers (see **Supplementary Table 5**) and Applied Biosystems Power SYBR Green PCR Master Mix (Thermo Scientific) in a Microamp EnduraPlate Optical 384 Well Clear Reaction Plate (Thermo Fisher Scientific) and the qPCR or RT-qPCR, respectively, was run on a QuantStudio 5 real-time PCR machine (Thermo Fisher Scientific). The *rpoC* gene was used as the housekeeping control for both the qPCR and RT-qPCR.

Measurement of evolvability

Twelve independent colonies for each strain were inoculated in a 96 well plate containing 200 μ l of fresh M63 at 37°C with shaking for 24 hours. The next day, 10 μ l of each was inoculated in 190 μ l of fresh M63 containing the appropriate concentration of DLX (0.75 μ g/ml or 2 μ g/ml for the data shown in **Figure 2**, and 0.55 μ g/ml or 0.32 μ g/ml for the data shown in **Figure 5**) and grown for 23 hours at 37°C with shaking. After 23 hours, OD₆₀₀ was measured and 10 μ l of each well was transferred to a 96-well plate containing 190 μ l of fresh M63 and DLX, and this was repeated for 5-14 days. The experiment was stopped if there was no growth for three consecutive days in any of the wells.

Determination of amplification stability

On day 1, strains were inoculated into fresh M63 media and grown for 24 hours at 37°C with shaking without DLX. On day 2, cells were diluted 1000-fold into tubes containing fresh media with no antibiotic or DLX at the appropriate concentrations. The same process was repeated for day 3, and for each strain there were two replicates. Genomic DNA was extracted each day, and whole-genome sequencing was performed. The *sdrM* copy number was determined as described above.

Determination of population heterogeneity of DLX resistance

Cells were grown overnight in MH2 broth supplemented with 1X ACGU, and the following day serial dilutions of the cultures were spotted on to MH2-agar plates supplemented with 1X ACGU, without DLX, or containing DLX at 2 µg/ml, 1 µg/ml, or 0.5 µg/ml and grown in a 37°C incubator overnight. The following day, colony forming units were determined.

Data Availability

The whole-genome sequencing data have been deposited at the NCBI Short Read Archive (SRA), associated with the BioProject PRJNA904786.

Acknowledgements

We would like to acknowledge the Center for Cancer Research Genomics Core for whole-genome sequencing library preparation and sequencing, and the Bose lab (University of Kansas Medical Center) for providing the pKK30 plasmid. We thank Susan Gottesman, Gigi Storz, John Dekker, and members of the Khare lab for comments on the manuscript, and members of the Gottesman, Ramamurthi, and Khare labs for discussion and suggestions throughout this work. This study utilized the computational resources of the NIH High Performance Computing Biowulf cluster (<http://hpc.nih.gov>). This work was supported by the Intramural Research Program of the NIH, National Cancer Institute, Center for Cancer Research.

References

1. Murray CJL, Ikuta KS, Sharara F, Swetschinski L, Robles Aguilar G, Gray A, et al. Global burden of bacterial antimicrobial resistance in 2019: a systematic analysis. *The Lancet*. 2022;399(10325):629-55.
2. Vestergaard M, Frees D, Ingmer H, Fischetti Vincent A, Novick Richard P, Ferretti Joseph J, et al. Antibiotic resistance and the MRSA problem. *Microbiology Spectrum*. 2019;7(2):7.2.18.
3. Boucher HW, Corey GR. Epidemiology of methicillin-resistant *Staphylococcus aureus*. *Clinical Infectious Diseases*. 2008;46(Supplement_5):S344-S9.
4. van Hal Sebastian J, Jensen Slade O, Vaska Vikram L, Espedido Björn A, Paterson David L, Gosbell Iain B. Predictors of mortality in *Staphylococcus aureus* bacteremia. *Clinical Microbiology Reviews*. 2012;25(2):362-86.
5. Bai AD, Lo CKL, Komorowski AS, Suresh M, Guo K, Garg A, et al. *Staphylococcus aureus* bacteraemia mortality: a systematic review and meta-analysis. *Clinical Microbiology and Infection*. 2022.
6. Klevens RM, Morrison MA, Nadle J, Petit S, Gershman K, Ray S, et al. Invasive methicillin-resistant *Staphylococcus aureus* infections in the United States. *JAMA*. 2007;298(15):1763-71.
7. Jernigan JA, Hatfield KM, Wolford H, Nelson RE, Olubajo B, Reddy SC, et al. Multidrug-resistant bacterial infections in U.S. hospitalized patients, 2012–2017. *New England Journal of Medicine*. 2020;382(14):1309-19.
8. Munita JM, Arias CA. Mechanisms of antibiotic resistance. *Microbiology Spectrum*. 2016;4(2).
9. Reygaert WC. An overview of the antimicrobial resistance mechanisms of bacteria. *AIMS Microbiology*. 2018;4(3):482-501.

10. Peterson E, Kaur P. Antibiotic resistance mechanisms in bacteria: relationships between resistance determinants of antibiotic producers, environmental bacteria, and clinical pathogens. *Frontiers in Microbiology*. 2018;9.
11. Du D, Wang-Kan X, Neuberger A, van Veen HW, Pos KM, Piddock LJV, et al. Multidrug efflux pumps: structure, function and regulation. *Nature Reviews Microbiology*. 2018;16(9):523-39.
12. Sandegren L, Andersson DI. Bacterial gene amplification: implications for the evolution of antibiotic resistance. *Nature Reviews Microbiology*. 2009;7(8):578-88.
13. Choby JE, Ozturk T, Abbott CN, Satola SW, Weiss DS. Heteroresistance via beta-lactamase gene amplification threatens the beta-lactam pipeline. *bioRxiv*. 2022:2022.06.07.494873.
14. Andersson DI, Hughes D. Gene amplification and adaptive evolution in bacteria. *Annual Review of Genetics*. 2009;43:167-95.
15. Oldfield E, Feng X. Resistance-resistant antibiotics. *Trends Pharmacol Sci*. 2014;35(12):664-74.
16. Nyerges A, Tomašič T, Durcik M, Revesz T, Szili P, Draskovits G, et al. Rational design of balanced dual-targeting antibiotics with limited resistance. *PLOS Biology*. 2020;18(10):e3000819.
17. Shukla R, Lavore F, Maity S, Derks MGN, Jones CR, Vermeulen BJA, et al. Teixobactin kills bacteria by a two-pronged attack on the cell envelope. *Nature*. 2022;608(7922):390-6.
18. Martin JK, 2nd, Sheehan JP, Bratton BP, Moore GM, Mateus A, Li SH, et al. A dual-mechanism antibiotic kills gram-negative bacteria and avoids drug resistance. *Cell*. 2020;181(7):1518-32.e14.
19. Ling LL, Schneider T, Peoples AJ, Spoering AL, Engels I, Conlon BP, et al. A new antibiotic kills pathogens without detectable resistance. *Nature*. 2015;517(7535):455-9.

20. Ince D, Zhang X, Silver LC, Hooper DC. Dual targeting of DNA gyrase and topoisomerase IV: target interactions of garenoxacin (BMS-284756, T-3811ME), a new desfluoroquinolone. *Antimicrobial Agents and Chemotherapy*. 2002;46(11):3370-80.
21. Ince D, Zhang X, Silver LC, Hooper DC. Topoisomerase targeting with and resistance to gemifloxacin in *Staphylococcus aureus*. *Antimicrobial Agents and Chemotherapy*. 2003;47(1):274-82.
22. Redgrave LS, Sutton SB, Webber MA, Piddock LJ. Fluoroquinolone resistance: mechanisms, impact on bacteria, and role in evolutionary success. *Trends in Microbiology*. 2014;22(8):438-45.
23. Candel FJ, Peñuelas M. Delafloxacin: design, development and potential place in therapy. *Drug Design Development and Therapy*. 2017;11:881-91.
24. Remy JM, Tow-Keogh CA, McConnell TS, Dalton JM, DeVito JA. Activity of delafloxacin against methicillin-resistant *Staphylococcus aureus*: resistance selection and characterization. *Journal of Antimicrobial Chemotherapy*. 2012;67(12):2814-20.
25. Ocheretyaner ER, Park TE. Delafloxacin: a novel fluoroquinolone with activity against methicillin-resistant *Staphylococcus aureus* (MRSA) and *Pseudomonas aeruginosa*. *Expert Review of Anti-Infective Therapy*. 2018;16(7):523-30.
26. Saravolatz LD, Stein GE. Delafloxacin: a new anti-methicillin-resistant *Staphylococcus aureus* fluoroquinolone. *Clinical Infectious Diseases*. 2019;68(6):1058-62.
27. Nilius AM, Shen LL, Hensey-Rudloff D, Almer LS, Beyer JM, Balli DJ, et al. In vitro antibacterial potency and spectrum of ABT-492, a new fluoroquinolone. *Antimicrobial Agents and Chemotherapy*. 2003;47(10):3260-9.
28. Iregui A, Khan Z, Malik S, Landman D, Quale J. Emergence of delafloxacin-resistant *Staphylococcus aureus* in Brooklyn, New York. *Clinical Infectious Diseases*. 2020;70(8):1758-60.

29. Noguchi N, Okihara T, Namiki Y, Kumaki Y, Yamanaka Y, Koyama M, et al. Susceptibility and resistance genes to fluoroquinolones in methicillin-resistant *Staphylococcus aureus* isolated in 2002. *Int J Antimicrob Agents*. 2005;25(5):374-9.
30. Vickers AA, O'Neill AJ, Chopra I. Emergence and maintenance of resistance to fluoroquinolones and coumarins in *Staphylococcus aureus*: predictions from in vitro studies. *J Antimicrob Chemother*. 2007;60(2):269-73.
31. Schmitz FJ, Jones ME, Hofmann B, Hansen B, Scheuring S, Lückefahr M, et al. Characterization of *griA*, *griB*, *gyrA*, and *gyrB* mutations in 116 unrelated isolates of *Staphylococcus aureus* and effects of mutations on ciprofloxacin MIC. *Antimicrobial Agents and Chemotherapy*. 1998;42(5):1249-52.
32. Yoon EJ, Lee CY, Shim MJ, Min YH, Kwon AR, Lee J, et al. Extended spectrum of quinolone resistance, even to a potential latter third-generation agent, as a result of a minimum of two GriA and two GyrA alterations in quinolone-resistant *Staphylococcus aureus*. *Chemotherapy*. 2010;56(2):153-7.
33. Yamada Y, Hideka K-i, Shiota S, Kuroda T, Tsuchiya T. Gene Cloning and Characterization of SdrM, a Chromosomally-Encoded Multidrug Efflux Pump, from *Staphylococcus aureus*. *Biological and Pharmaceutical Bulletin*. 2006;29(3):554-6.
34. Lu S, Wang J, Chitsaz F, Derbyshire MK, Geer RC, Gonzales NR, et al. CDD/SPARCLE: the conserved domain database in 2020. *Nucleic acids research*. 2020;48(D1):D265-D8.
35. Varadi M, Anyango S, Deshpande M, Nair S, Natassia C, Yordanova G, et al. AlphaFold Protein Structure Database: massively expanding the structural coverage of protein-sequence space with high-accuracy models. *Nucleic Acids Research*. 2022;50(D1):D439-d44.
36. Jumper J, Evans R, Pritzel A, Green T, Figurnov M, Ronneberger O, et al. Highly accurate protein structure prediction with AlphaFold. *Nature*. 2021;596(7873):583-9.

37. Siala W, Mingeot-Leclercq M-P, Tulkens Paul M, Hallin M, Denis O, Van Bambeke F. Comparison of the Antibiotic Activities of Daptomycin, Vancomycin, and the Investigational Fluoroquinolone Delafloxacin against Biofilms from *Staphylococcus aureus* Clinical Isolates. *Antimicrobial Agents and Chemotherapy*. 2014;58(11):6385-97.
38. Floyd JL, Smith KP, Kumar SH, Floyd JT, Varela MF. LmrS is a multidrug efflux pump of the major facilitator superfamily from *Staphylococcus aureus*. *Antimicrobial agents and chemotherapy*. 2010;54(12):5406-12.
39. Narui K, Noguchi N, Wakasugi K, Sasatsu M. Cloning and characterization of a novel chromosomal drug efflux gene in *Staphylococcus aureus*. *Biological and Pharmaceutical Bulletin*. 2002;25(12):1533-6.
40. Szklarczyk D, Gable AL, Nastou KC, Lyon D, Kirsch R, Pyysalo S, et al. The STRING database in 2021: customizable protein–protein networks, and functional characterization of user-uploaded gene/measurement sets. *Nucleic acids research*. 2021;49(D1):D605-D12.
41. Krute CN, Krausz KL, Markiewicz MA, Joyner JA, Pokhrel S, Hall PR, et al. Generation of a stable plasmid for *in vitro* and *in vivo* studies of *Staphylococcus* species. *Applied and environmental microbiology*. 2016;82(23):6859-69.
42. Andersson DI, Nicoloff H, Hjort K. Mechanisms and clinical relevance of bacterial heteroresistance. *Nature Reviews Microbiology*. 2019;17(8):479-96.
43. Nicoloff H, Hjort K, Levin BR, Andersson DI. The high prevalence of antibiotic heteroresistance in pathogenic bacteria is mainly caused by gene amplification. *Nature Microbiology*. 2019;4(3):504-14.
44. Rahman T, Yarnall B, Doyle DA. Efflux drug transporters at the forefront of antimicrobial resistance. *European Biophysics Journal*. 2017;46(7):647-53.
45. Dashtbani-Roozbehani A, Brown MH. Efflux pump mediated antimicrobial resistance by *Staphylococci* in health-related environments: challenges and the quest for inhibition. *Antibiotics*. 2021;10(12).

46. Lekshmi M, Ammini P, Adjei J, Sanford LM, Shrestha U, Kumar S, et al. Modulation of antimicrobial efflux pumps of the major facilitator superfamily in *Staphylococcus aureus*. *AIMS Microbiology*. 2018;4(1):1-18.
47. Ohshita Y, Hiramatsu K, Yokota T. A point mutation in *norA* gene is responsible for quinolone resistance in *Staphylococcus aureus*. *Biochemical and Biophysical Research Communications*. 1990;172(3):1028-34.
48. Floyd JL, Smith KP, Kumar SH, Floyd JT, Varela MF. LmrS is a multidrug efflux pump of the major facilitator superfamily from *Staphylococcus aureus*. *Antimicrobial Agents and Chemotherapy*. 2010;54(12):5406-12.
49. Narui K, Noguchi N, Wakasugi K, Sasatsu M. Cloning and characterization of a novel chromosomal drug efflux gene in *Staphylococcus aureus*. *Biological and Pharmaceutical Bulletin*. 2002;25(12):1533-6.
50. Truong-Bolduc QC, Wang Y, Chen C, Hooper DC. Transcriptional regulator TetR21 controls the expression of the *Staphylococcus aureus* LmrS efflux pump. *Antimicrobial Agents and Chemotherapy*. 2017;61(8).
51. Fernández L, Hancock RE. Adaptive and mutational resistance: role of porins and efflux pumps in drug resistance. *Clinical Microbiology Reviews*. 2012;25(4):661-81.
52. Baylay AJ, Ivens A, Piddock LJ. A novel gene amplification causes upregulation of the PatAB ABC transporter and fluoroquinolone resistance in *Streptococcus pneumoniae*. *Antimicrobial Agents and Chemotherapy*. 2015;59(6):3098-108.
53. López-Causapé C, Sommer LM, Cabot G, Rubio R, Ocampo-Sosa AA, Johansen HK, et al. Evolution of the *Pseudomonas aeruginosa* mutational resistome in an international Cystic Fibrosis clone. *Scientific Reports*. 2017;7(1):5555.
54. Li Y, Ge X. Discovering interrelated natural mutations of efflux pump KmrA from *Klebsiella pneumoniae* that confer increased multidrug resistance. *Protein Science*. 2022;31(6):e4323.

55. Lyu M, Moseng MA, Reimche JL, Holley CL, Dhulipala V, Su CC, et al. Cryo-EM structures of a gonococcal multidrug efflux pump illuminate a mechanism of drug recognition and resistance. *mBio*. 2020;11(3).
56. El Meouche I, Dunlop MJ. Heterogeneity in efflux pump expression predisposes antibiotic-resistant cells to mutation. *Science*. 2018;362(6415):686-90.
57. Bhattacharyya S, Bhattacharyya M, Pfannenstiel DM, Nandi AK, Hwang Y, Ho K, et al. Efflux-linked accelerated evolution of antibiotic resistance at a population edge. *Molecular Cell*. 2022;82(22):4368-85.e6.
58. Nolivos S, Cayron J, Dedieu A, Page A, Delolme F, Lesterlin C. Role of AcrAB-TolC multidrug efflux pump in drug-resistance acquisition by plasmid transfer. *Science*. 2019;364(6442):778-82.
59. Papkou A, Hedge J, Kapel N, Young B, MacLean RC. Efflux pump activity potentiates the evolution of antibiotic resistance across *S. aureus* isolates. *Nature Communications*. 2020;11(1):3970.
60. Iregui A, Khan Z, Malik S, Landman D, Quale J. Emergence of Delafloxacin-Resistant *Staphylococcus aureus* in Brooklyn, New York. *Clin Infect Dis*. 2020;70(8):1758-60.
61. Albertson DG. Gene amplification in cancer. *Trends in Genetics*. 2006;22(8):447-55.
62. Levine C, Hiasa H, Marians KJ. DNA gyrase and topoisomerase IV: biochemical activities, physiological roles during chromosome replication, and drug sensitivities. *Biochimica et Biophysica Acta*. 1998;1400(1-3):29-43.
63. Drlica K. Mechanism of fluoroquinolone action. *Current Opinion in Microbiology*. 1999;2(5):504-8.
64. Hashimi SM, Wall MK, Smith AB, Maxwell A, Birch RG. The phytotoxin albicidin is a novel inhibitor of DNA gyrase. *Antimicrobial Agents and Chemotherapy*. 2007;51(1):181-7.

65. Saathoff M, Kosol S, Semmler T, Tedin K, Dimos N, Kupke J, et al. Gene amplifications cause high-level resistance against albicidin in Gram-negative bacteria. *bioRxiv*. 2022:2022.09.15.507240.
66. Pardee AB, Jacob F, Monod J. The genetic control and cytoplasmic expression of “Inducibility” in the synthesis of β -galactosidase by *E. coli*. *Journal of Molecular Biology*. 1959;1(2):165-78.
67. Khare A, Tavazoie S. Multifactorial competition and resistance in a two-species bacterial system. *PLOS Genetics*. 2015;11(12):e1005715.
68. Chen S, Zhou Y, Chen Y, Gu J. fastp: an ultra-fast all-in-one FASTQ preprocessor. *Bioinformatics*. 2018;34(17):i884-i90.
69. Martin M. Cutadapt removes adapter sequences from high-throughput sequencing reads. *EMBnet Journal*. 2011;17(1):10-2.
70. Bolger AM, Lohse M, Usadel B. Trimmomatic: a flexible trimmer for Illumina sequence data. *Bioinformatics*. 2014:btu170.
71. Deatherage DE, Barrick JE. Identification of mutations in laboratory-evolved microbes from next-generation sequencing data using breseq. In: Sun L, Shou W, editors. *Engineering and Analyzing Multicellular Systems. Methods in Molecular Biology*: Springer; 2014. p. 165-88.
72. Schuster CF, Howard SA, Grundling A. Use of the counter selectable marker PheS* for genome engineering in *Staphylococcus aureus*. *Microbiology* 2019;165(5):572-84.
73. Monk IR, Tree JJ, Howden BP, Stinear TP, Foster TJ. Complete bypass of restriction systems for major *Staphylococcus aureus* lineages. *mBio*. 2015;6(3):e00308-15.
74. R.J.W. Lambert JP. Susceptibility testing: accurate and reproducible minimum inhibitory concentration (MIC) and non-inhibitory concentration (NIC) values. *Journal of Applied Microbiology*. 2000;88:784-90.

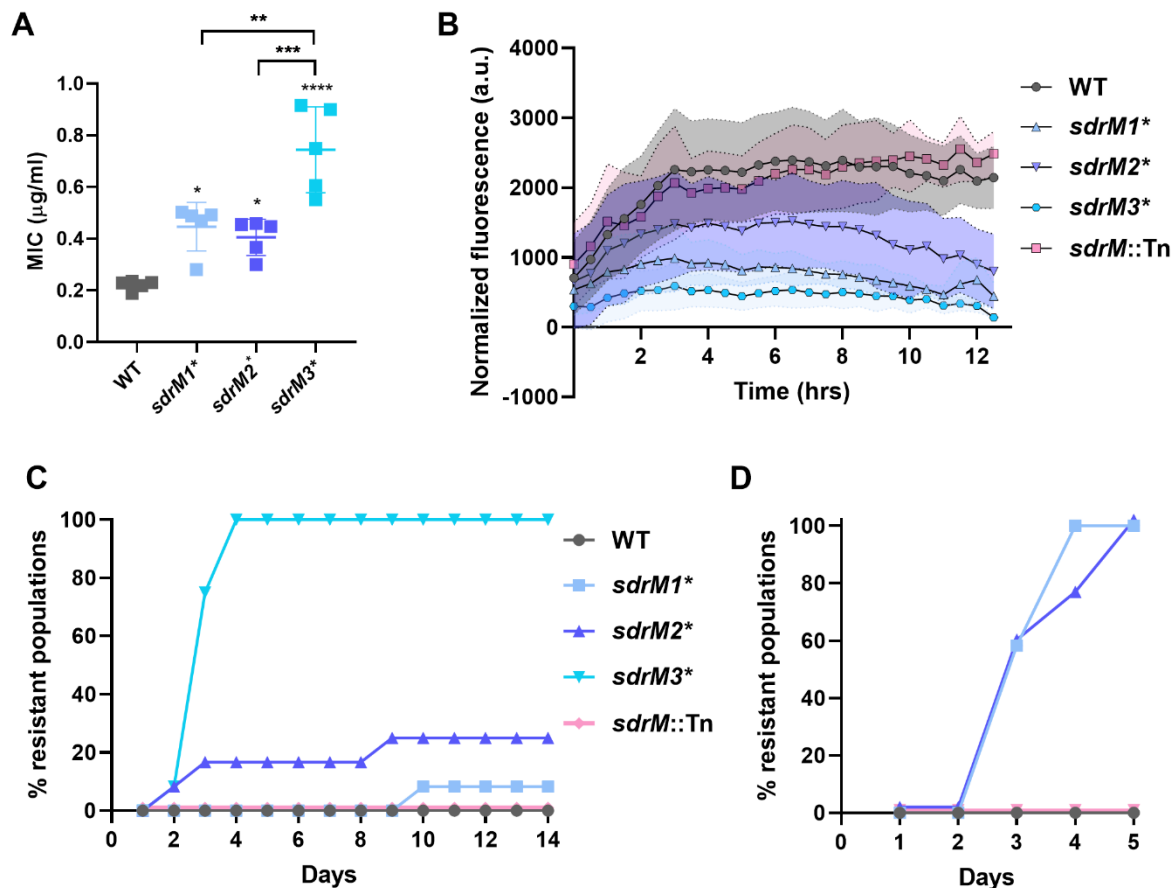


Figure 2. Evolved *sdrM* alleles increase DLX resistance and evolvability. (A) DLX MICs of WT, and the three *sdrM* allelic replacement mutants in M63. Error bars show the standard deviation of five biological replicates. Significance is shown for comparison to the WT, or between mutants as indicated, as tested by a one-way ANOVA with Tukey's test for multiple comparisons (* $p < 0.05$, ** $p < 0.01$, *** $p < 0.001$, **** $p < 0.0001$). **(B)** Normalized fluorescence (intrinsic fluorescence of DLX / OD₆₀₀) was measured for the indicated strains, as a proxy for the intracellular DLX concentration. The shaded areas represent the standard error of three biological replicates. **(C, D)** Percentage of the 12 independent populations of the indicated strains that evolved DLX resistance over time in **(C)** 2 µg/ml DLX or **(D)** 0.75 µg/ml DLX. Since the DLX MIC of the *sdrM3** strain is ~0.75 µg/ml, this strain was not included in **(D)**.

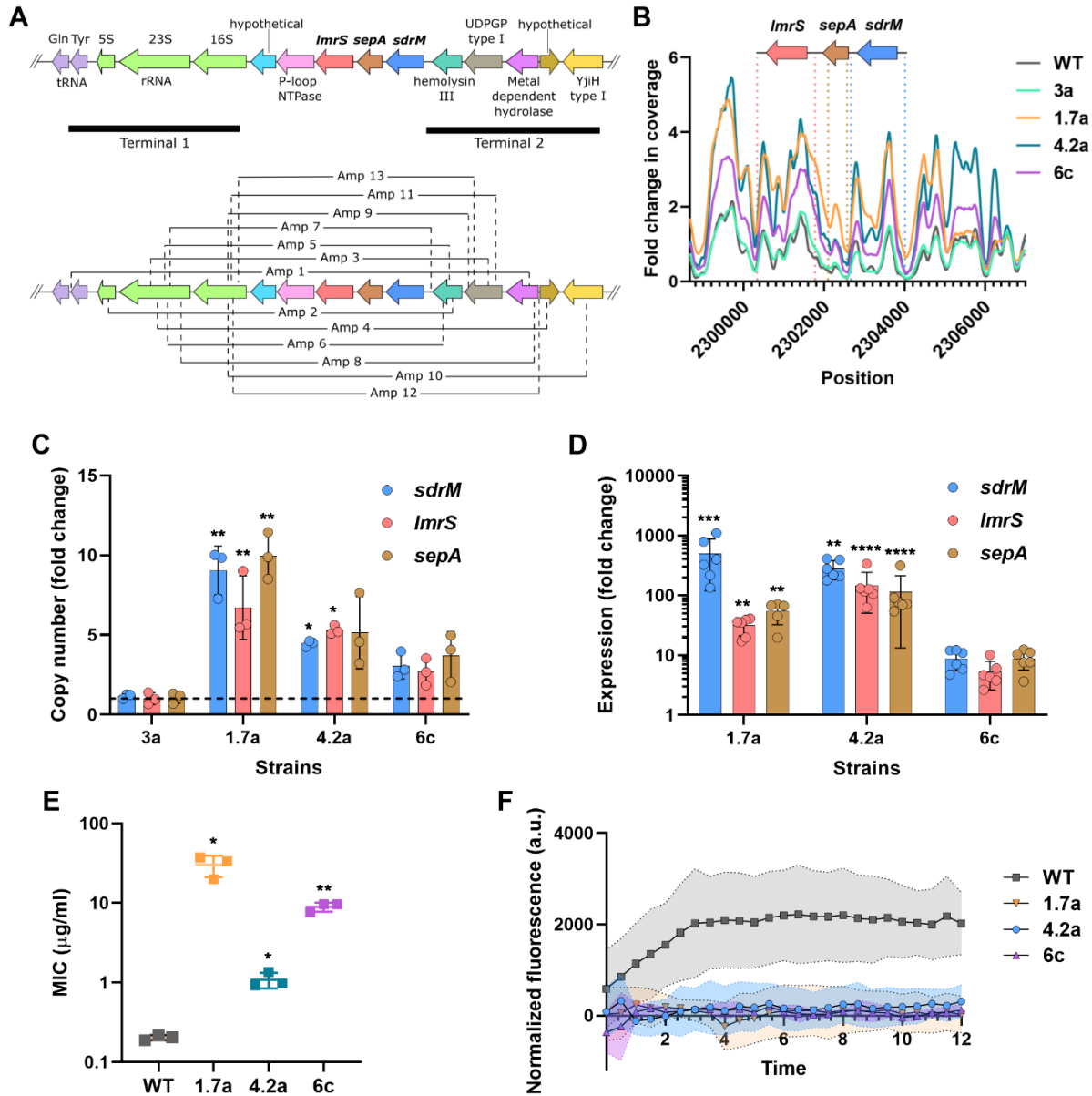


Figure 3. Evolved mutants with gene amplifications have high efflux pump expression and DLX resistance. (A) The *sdrM* genomic locus and the 13 distinct types of efflux pump gene amplifications seen in the evolved populations. The regions containing the two ends of the amplification in all cases are shown (Terminals 1 and 2). **(B)** Relative read coverage of the amplified regions compared to the entire genome for the indicated strains. The lines represent a smoothed fit using a generalized additive model considering the nearest 100 neighbors. **(C)** Fold-

change of the copy number of *sdrM*, *lmrS* and *sepA* in the indicated strains compared to the WT as measured by qPCR of genomic DNA. Error bars show the standard deviation of three technical replicates. **(D)** Fold-change in expression of *sdrM*, *lmrS*, and *sepA* in the indicated strains compared to WT, as measured by RT-qPCR. Error bars show the standard deviation of three technical replicates each from two biological replicates. **(E)** DLX MICs of the indicated strains in M63. Error bars show the standard deviation of three biological replicates. **(F)** Normalized fluorescence (intrinsic fluorescence of DLX / OD₆₀₀) of the indicated strains, as a proxy for the intracellular DLX concentration. The shaded areas represent the standard error of three biological replicates. Significance is shown for comparison to **(C-D)** WT value set to 1 as tested by a Kruskal-Wallis test followed by an uncorrected Dunn's test for each comparison and **(E)** WT as tested by Brown-Forsythe and Welch ANOVA tests, followed by an unpaired t-test with Welch's correction for each comparison (* $p < 0.05$, ** $p < 0.01$, *** $p < 0.001$, **** $p < 0.0001$).

6c

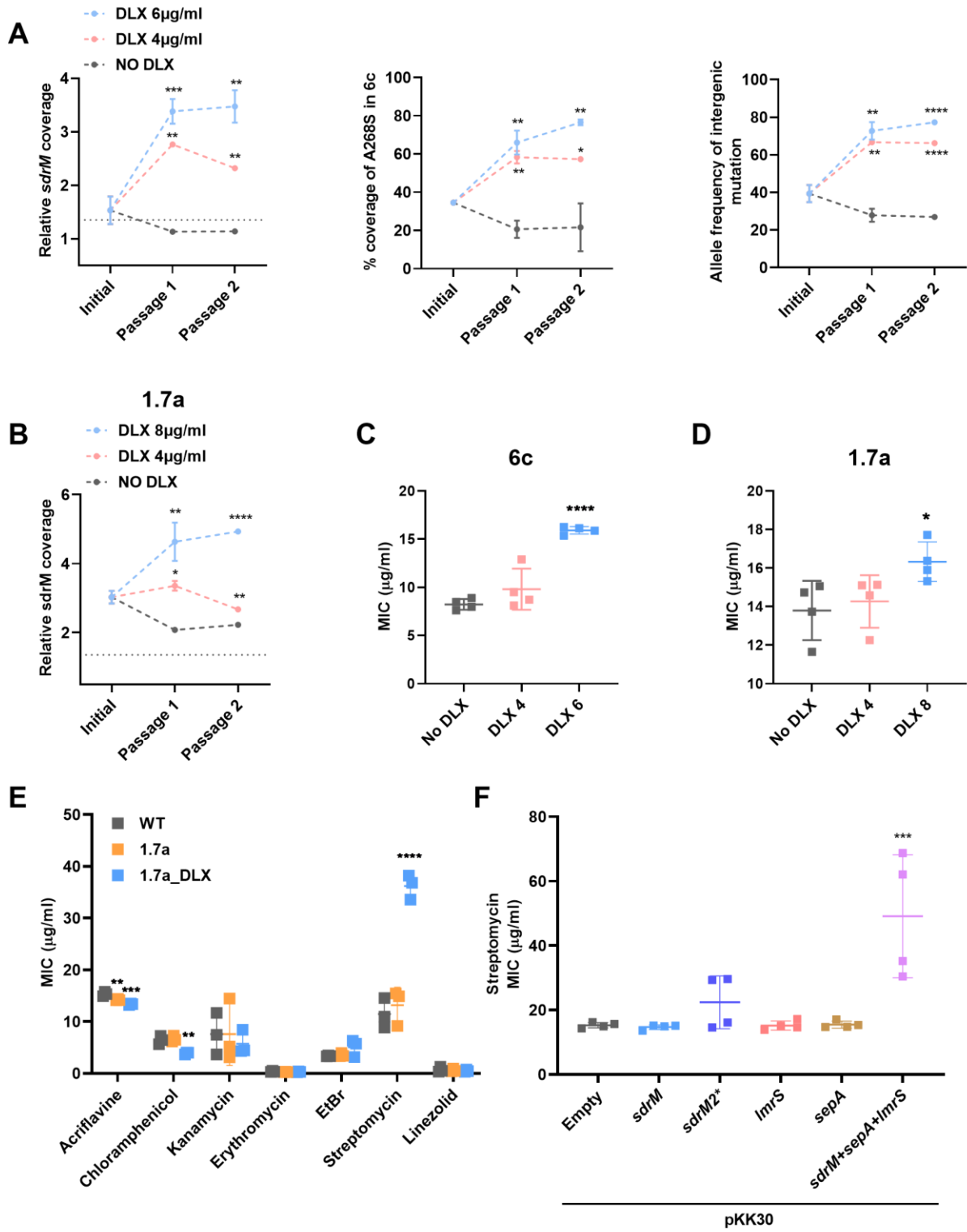


Figure 4. Increased copy number of efflux pump amplification leads to cross-resistance.

(A) Copy number of *sdrM* and the allele frequencies of the two mutations that constitute the *sdrM3** allele in 6c upon passaging in either no DLX media, or two concentrations of DLX. **(B)** Copy number of *sdrM* in 1.7a upon passaging in either no DLX media, or two concentrations of DLX. Error bars show the standard deviation from two independent passaging experiments **(C, D)** DLX MICs in M63 of 6c and 1.7a populations after the second passage in either no DLX, or **(C)** 4µg/ml DLX (DLX 4) or 6µg/ml DLX (DLX 6) for 6c and **(D)** 4µg/ml DLX (DLX 4) or 8µg/ml DLX (DLX 8) for 1.7a. Error bars show the standard deviation of two biological replicates each from two independent passaging experiments. **(E)** MICs of WT, 1.7a, or 1.7a grown overnight in 2µg/ml DLX (1.7a_DLX) in the indicated antibiotics in MH2. Error bars show the standard deviation of three biological replicates. **(F)** Streptomycin MICs of the pKK30-overexpression strains in MH2. Error bars show the standard deviation of four biological replicates. Significance is shown for comparison to **(A-D)** the respective no DLX control, **(E)** WT and **(F)** the strain carrying the empty vector, as tested by **(A-D, F)** a one-way ANOVA with the Holm-Sidak's test for multiple comparisons and **(E)** an unpaired t-test followed by correction for multiple comparisons using the Holm-Sidak method (* $p < 0.05$, ** $p < 0.01$, *** $p < 0.001$, **** $P < 0.0001$).

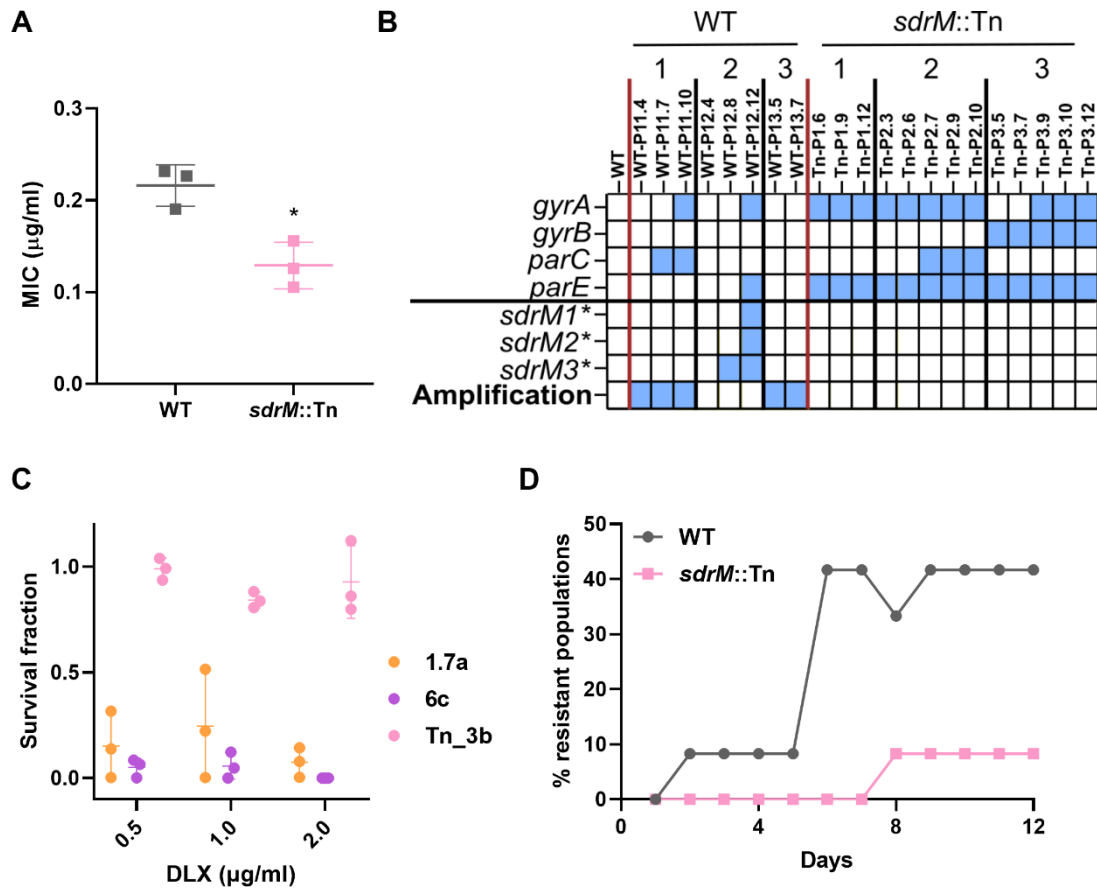


Figure 5. The presence of *sdrM* facilitates the evolution of DLX resistance. (A) DLX MICs of the WT and *sdrM::Tn* strains in M63. The error bars show the standard deviation of three biological replicates. Significance is shown for comparison to the WT as tested by an unpaired t-test (* $p < 0.05$). **(B)** The presence of mutations in genes encoding DNA gyrase subunits (*gyrA*, *gyrB*) and DNA topoisomerase IV subunits (*parC*, *parE*), the three mutant alleles *sdrM1**, *sdrM2** and *sdrM3**, and a genomic amplification containing *sdrM*, are shown for populations from intermediate passages of three independently evolved populations each of the WT and *sdrM::Tn* strains. **(C)** The survival fraction for the indicated strains in multiple DLX concentrations compared to a no DLX control, measured as cfu/ml on the respective plates. Error bars represent the standard deviation of three biological replicates. **(D)** Percentage of the 12 independent populations of the indicated strains that evolved DLX resistance over time in 2.5x the respective DLX MICs (0.55 μg/ml for the WT and 0.32 μg/ml for *sdrM::Tn*).